Nuclear Instruments and Methods in Physics Research A 745 (2014) 1–6

Contents lists available at ScienceDirect

Nuclear Instruments and Methods in Physics Research A

journal homepage: www.elsevier.com/locate/nima

Results on damage induced by high-energy protons in LYSO calorimeter crystals

G. Dissertori [a], D. Luckey [a,1], F. Nessi-Tedaldi [a,*], F. Pauss [a], M. Quittnat [a], R. Wallny [a], M. Glaser [b]

[a] Institute for Particle Physics, ETH Zurich, 8093 Zurich, Switzerland
[b] CERN - PH Department, 1211 Geneva 23, Switzerland

ARTICLE INFO

Article history:
Received 10 September 2013
Received in revised form
13 December 2013
Accepted 3 February 2014
Available online 8 February 2014

Keywords:
Crystal
Calorimeter
Hadron
Damage
Scintillator

ABSTRACT

Lutetium-Yttrium Orthosilicate doped with Cerium (LYSO), as a bright scintillating crystal, is a candidate for calorimetry applications in strong ionising-radiation fields and large high-energy hadron fluences are expected at the CERN Large Hadron Collider after the planned High-Luminosity upgrade. There, proton–proton collisions will produce fast hadron fluences up to $\sim 5 \times 10^{14}$ cm^{-2} in the large-rapidity regions of the calorimeters.

The performance of LYSO has been investigated, after exposure to different fluences of 24 GeV c^{-1} protons. Measured changes in optical transmission as a function of proton fluence are presented, and the evolution over time due to spontaneous recovery at room temperature is studied.

The activation of materials will also be an issue in the described environment. Studies of the ambient dose induced by LYSO and its evolution with time, in comparison with other scintillating crystals, have also been performed through measurements and FLUKA simulations.

1. Introduction

The planned upgrade to High-Luminosity running of the Large Hadron Collider at CERN (HL-LHC) will impose performance requirements on detectors that are more stringent than those adopted for LHC construction two decades ago. According to the present schedule, such an upgrade should start in 2022. Some of the detectors envisage an upgrade, primarily of their end caps, and materials suitable for that challenging environment need to be swiftly identified. If adopted for electromagnetic calorimetry, inorganic scintillators will have to perform adequately in an environment where ionising radiation levels can be as high as 65 Gy h^{-1}, and energetic hadron fluences are expected to reach integrated values of 5×10^{14} cm^{-2}.

The present work extends our earlier studies of Lead Tungstate [1–4] and Cerium Fluoride (CeF_3 [5]), to explore potentially suitable scintillators. Therein, we have shown how Lead Tungstate ($PbWO_4$) exposed to hadronic showers from high-energy protons and pions experiences a cumulative loss of light transmission which is permanent at room temperature, while no hadron-specific change in scintillation emission was observed. The amplitude of the damage can reach values unsuitable for running at the HL-LHC [6,7]. A microscopic investigation [4] has allowed us to ascribe the dominant damage mechanism to heavy fragments arising from Lead and Tungsten fission, which can have energy losses of up to $\mathcal{O}(10^5$ MeV cm$^{-1})$ along their tracks, which range up to 10 μm. In the regions around these tracks the lattice structure is left strained, disordered, or re-oriented. These damage regions have different optical and mechanical properties compared to the surrounding crystal lattice, and they can act as scatterers for light propagating in the crystal, thus affecting the light transmission.

The qualitative understanding we gained of hadron damage in Lead Tungstate led to the prediction [8] that such hadron-specific damage contributions are absent in crystals consisting only of elements with $Z < 71$, which is the experimentally observed threshold for fission [9], while they should be expected in crystals containing elements with $Z > 71$. We confirmed the first prediction with measurements [5] that show how hadrons in CeF_3 cause a damage that recovers at room temperature, with none of the features present that we observed for $PbWO_4$, thus making it an excellent candidate for HL-LHC applications. The second prediction is confirmed by existing proton-damage measurements in BGO [10,11], in Lead Fluoride and in BSO [12], which all contain elements with $Z > 71$.

All this evidence leads to the guideline that for resistance to damage from energetic hadrons, materials need to consist of elements not exceeding $Z=71$. In the light of all this, Cerium-doped Lutetium-Yttrium Orthosilicate (briefly LYSO), which is a

* Correspondence to: CERN - PH Department, 1211 Geneva 23, Switzerland.
E-mail address: Francesca.Nessi-Tedaldi@cern.ch (F. Nessi-Tedaldi).
[1] Also at Massachusetts Institute of Technology, Cambridge, MA, USA.

http://dx.doi.org/10.1016/j.nima.2014.02.003
0168-9002/

commercially available scintillator, is of crucial interest, since it contains Lutetium, that with Z=71 sits right at the threshold for fission. For this reason, and for all the further characteristics described in Section 2, this study addresses the effect of energetic hadrons on the performance of LYSO scintillating crystals. Its outcome is a highly relevant input to decisions on calorimeter technology for HL-LHC running and for further applications where an exposure to intense fluxes of energetic hadrons has to be taken into account.

2. LYSO

Cerium-doped silicate-based crystals were recently developed for medical applications. Initially, Cerium-doped Lutetium Orthosilicate (Lu_2SiO_5:Ce, or briefly LSO) was first investigated as a phosphor for cathode ray tube displays [13], then rediscovered as a promising scintillator and first grown in 1989 [14]. A mass-production was later established for LSO [15] and for LYSO [16] in the early years 2000. LYSO is a mixed crystal, a dense, bright scintillator, which is nowadays commercially available, being industrially produced by several companies for high-precision Positron-Emission Tomography. Its chemical formula is $Ce_{2x}(Lu_{1-y}Y_y)_{2(1-x)}SiO_5$, where for crystals produced by the Shanghai Institute of Ceramics (SIC, [17]) $x=0.0015$ [18], while for St. Gobain crystals [19] it is only known to be less than 0.01 [20], along with $y=0.1$ for both mentioned producers. Its density ($\rho=$ 7.4 g cm^{-3}), radiation length ($X_0=1.14$ cm), Molière radius ($R_M=2.07$ cm), nuclear interaction length ($\lambda_I=20.9$ cm) and refractive index ($n=1.82$) make it a competitive medium for compact calorimeters. Its emission is centred at 430 nm [21], with a decay time constant of 40 ns; it is rather insensitive to temperature changes (dLY/dT (20 °C)$=-0.2\%$ per °C) as well as bright (85% of NaI($T\ell$)) and thus suitable for high-rate, high-precision calorimetry. Large prototype crystals were initially observed exhibiting inhomogeneities in light yield and transmission, but this has recently been demonstrated to be a solvable issue [22]. Furthermore, calorimeter designs being considered for HL-LHC detector upgrades rather envisage sampling options, where such inhomogeneities are no issue, due to the small size of the individual scintillator elements involved [7].

LYSO contains a fraction of the naturally occurring isotope ^{176}Lu, which undergoes β-decay followed by the emission of 88, 202 and 307 keV γ-rays, causing signals which can be assimilated to phosphorescence. These can be exploited for calibration purposes, in that the energy deposition of the concomitant γ rays, that add to the continuum due to the β-decay, produces a peculiar pattern [23], whose shape slightly varies depending on the crystal dimensions, since these affect the γ energy deposition containment.

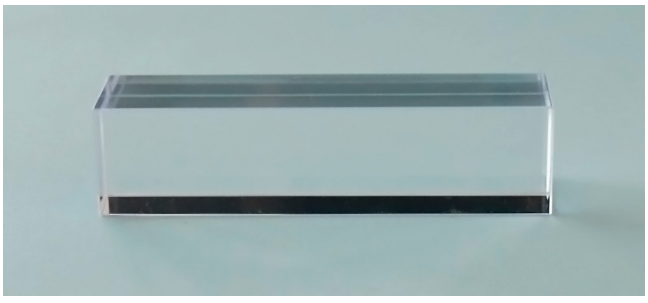

Fig. 1. One of the tested LYSO samples, showing excellent mechanical processing and optical surface treatment.

Numerous studies of LYSO characteristics have been performed, as can be gathered in Ref. [21]. The performance under γ-irradiation was thoroughly investigated [24], γ-radiation effects have been shown to be small and dose rate dependent, with no recovery at ambient temperature. The performance for precision calorimetry [25] is such that attractive energy resolutions are achieved for photons between 200 and 500 MeV along with a time resolution as good as 150 ps. The capability to be grown in large ingots, needed for medium- and high-energy calorimetry, has been demonstrated [26] and the properties of such large samples have been studied [21]. The main concern about LYSO procurement remains the cost linked to raw materials, in that Lutetium is a rare-earth. Its performance when exposed to large fluxes of energetic hadrons, was so far unexplored. It is crucial for applications such as calorimetry at the HL-LHC and it is the subject of the study presented herein.

3. Experimental setup

The two LYSO samples used for this test were produced one by Saint-Gobain that commercialises LYSO under the name PreLude420 and one by SIC. The samples have dimensions $25\times 25\times 100$ mm^3, corresponding to 8.8 X_0 in length (Fig. 1).

The irradiations of individual samples were performed at the IRRAD1 irradiation facility of the CERN PS T7 beam line [27] with 24 GeV c^{-1} protons, up to different fluences representative for HL-LHC running conditions. The proton beam was widened in order to uniformly irradiate the whole crystal front face. A list of the irradiations performed is listed in Table 1. It might be worth noting, for comparison, that from HL-LHC running up to an integrated luminosity of 3000 fb^{-1}, at a pseudorapidity $\eta=2.6$ e.g., a hadron fluence of 2×10^{14} cm^{-2} and an average particle energy of the order of 1 GeV are expected from simulations [7,28]. After each irradiation, the samples were stored in the dark, at ambient temperature, and periodic measurements of the light transmission were performed, where the earliest measurements were taken when sample activation allowed for safe handling, according to the regulations for radioprotection. This corresponded to 20, 110 and respectively 60 days after the first, second, and third irradiation. The dosimetry for all irradiations was performed using the known activation cross-section of Aluminium foils placed in front of the sample during irradiation [1].

4. Visual observations

While a slight loss of light transmission is barely visible through the naked eye in ambient light on the tested crystals, it is possible to observe modifications due to the irradiation, by shining a collimated beam of light through the samples. This was

Table 1
Detailed list of the irradiations performed.

Irradiation date	Sample origin	p fluence (cm^{-2})	p flux (cm^{-2} h^{-1})
June 2009	SIC	$\Phi_1^p=(8.85\pm0.62)\times10^{12}$	$\phi_1^p=(5.97\pm0.42)\times10^{12}$
November 2010	SIC	$\Phi_2^p=(7.24\pm0.54)\times10^{13}$	$\phi_2^p=(3.82\pm0.29)\times10^{12}$
July 2011	St. Gobain	$\Phi_3^p=(2.07\pm0.16)\times10^{13}$	$\phi_3^p=(5.67\pm0.43)\times10^{12}$

performed using a green LASER beam of 543.5 nm wavelength. In the photograph of Fig. 2, one can observe how the beam of green LASER light becomes visible when it traverses one of the proton-irradiated samples. This phenomenon was already observed in proton-irradiated $PbWO_4$ crystals [1,4], where it is very pronounced. As for $PbWO_4$, by placing a Polaroid filter between the right half of the LYSO crystal and the camera, we observe cancellation, proving that the scattered light is polarised. This feature has been linked, in our previous studies cited above, to Rayleigh scattering off small regions with different optical properties, as can be caused by disorder induced by hadron damage. We conclude that at least a small fraction of the damage is due to light scattered off localised regions of damage, as it is the case for $PbWO_4$, where the presence of such regions, also called "fission tracks" in the literature, have been recently visualised [4]. This visualisation in $PbWO_4$ confirmed our understanding, first gained through indirect evidence, of the mechanism at work: the large energy deposits of fission fragments.

Lutetium, with Z=71, is right at the threshold for fission [9], and the relatively smaller probability for it to happen might explain why the effect is less pronounced here than what observed in $PbWO_4$.

5. Changes in light transmission

To quantify the loss of light transmission induced by hadrons, we have measured it as a function of wavelength, in 1 nm steps, with a high-precision Lambda900 spectrophotometer from Perkin-Elmer [29]. The resulting transmission curves before irradiation and at selected times after irradiation, are visible in Fig. 3, uncorrected for Fresnel losses. Systematic drifts in the instrument calibration and in the positioning accuracy affect the data with an overall systematic uncertainty that amounts at most to 0.8% below the transmission band edge, and to 0.5% above, according to a detailed study performed in Ref. [1].

One can observe how the loss of transmission is smooth, and how the typical dips related to color centres are absent. This indicates that color center formation—as typical for ionising damage—is not the main damage mechanism here. Transmission curves taken at different intervals after irradiation are superposed, indicating that the loss does not recover at room temperature, over a time span of 1 year or longer. For this reason, in later plots we do not quote any further the time after irradiation of the measurements.

We have determined the induced absorption $\mu_{IND}(\lambda)$ as a function of wavelength λ, that is defined as

$$\mu_{IND}(\lambda) = \frac{1}{L} \times \ln \frac{LT0(\lambda)}{LT(\lambda)} \quad (1)$$

with L being the crystal length and $LT0$ (LT) being the light transmission before (after) irradiation. The measurements for the three irradiations are presented in Fig. 4. There, the precision on the μ_{IND} determination is derived from Eq. (1) and from the uncertainties on light transmission measurements, to be affected by a systematic uncertainty of 0.08 m^{-1} at 400 nm, steadily increasing with wavelength to reach 0.17 m^{-1} at 600 nm, remaining then constant for higher wavelengths. The comparison in Fig. 4, between the data for the three fluences, indicates proportionality between damage and Φ^p. A small, unexplained, deviation from a scaling behaviour is observed between samples for $\lambda > 550$ nm, that is however far from the range of wavelengths relevant for the scintillation light collection, and might be interesting to

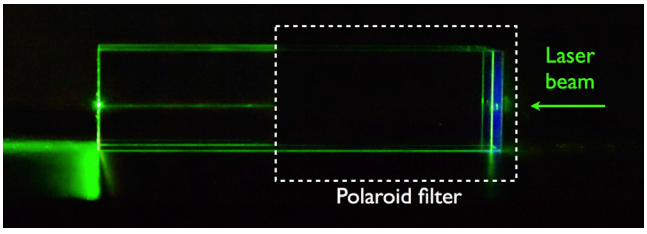

Fig. 2. A faint beam reveals the 543.5 nm green Laser light shone through a proton-irradiated LYSO crystal and thus indicates the presence of scatterers. Cancellation by a Polaroid filter (placement outlined by a dashed white rectangle) indicates that the scattered light is polarised. (For interpretation of the references to color in this figure legend, the reader is referred to the web version of this article.)

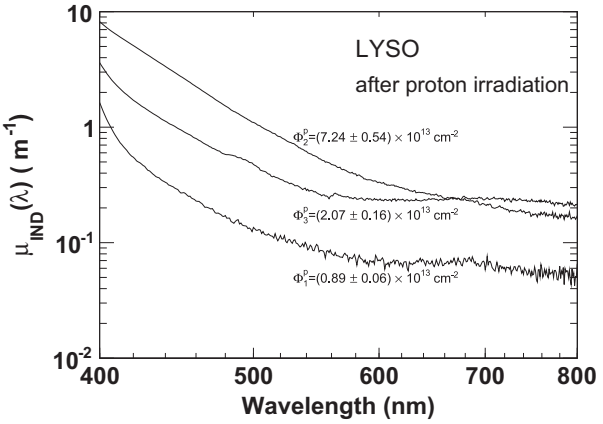

Fig. 4. Induced absorption as a function of wavelength, measured longitudinally through the 100 mm length of the SIC crystal after each of the two irradiations with fluences Φ_1^p and Φ_2^p, and for the St. Gobain crystal after the irradiation with fluence Φ_3^p. The uncertainties on the measurements are discussed in the text.

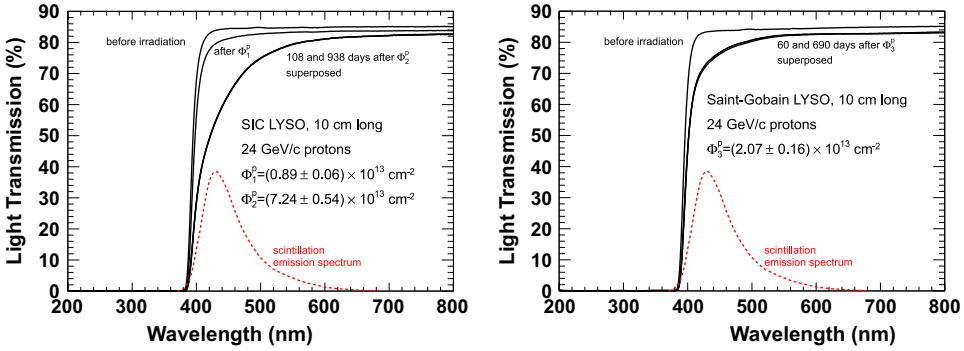

Fig. 3. Light transmission as a function of wavelength, measured longitudinally through the 100 mm length of the crystals. Left: values before irradiation and at two different times after the irradiations with fluences Φ_1^p and Φ_2^p for the SIC sample, along with the scintillation emission spectrum from Ref. [21]. Right: values before and at two different times after irradiation with fluence Φ_3^p for the St. Gobain sample (emission spectrum as above). The uncertainties on the measurements are addressed in the text.

investigate in future studies. The smoothness of the data curves confirms the absence of dominant color centers. Their slope is shallower than for $PbWO_4$ [1], where a λ^{-4} behaviour was observed, typical for Rayleigh scattering. This latter observation indicates that, although the creation of some scattering centres through hadrons must have occurred, as illustrated in Section 4, their presence is by far not the dominant mechanism to explain the loss of light transmission.

Measurements of the induced absorption at different time intervals after irradiation are presented in Fig. 5, where values are shown at 430 nm, the peak-of-emission wavelength. No significant recovery is observed, thus implying a long-term damage that is permanent at room temperature, when observed over several months and even years after irradiation.

For the LYSO evaluation as a possible alternative scintillator to be used at the HL-LHC, it is useful to compare its level of damage, quantified as the induced absorption at the peak-of-emission wavelength, with the ones of $PbWO_4$ and CeF_3 as a function of integrated proton fluence. This is done in Fig. 6, where the central data point for LYSO corresponds to the crystal produced by St. Gobain, the other ones to the two irradiation tests of the SIC crystal. The plot shows how the damage in LYSO is cumulative, similar to what observed for $PbWO_4$. However, a fit to the data shows how the damage amplitude for LYSO is everywhere a factor 4.5 smaller than what was measured in $PbWO_4$. The values for CeF_3 instead recover and their value depends on the time elapsed after irradiation [5].

The observed trend further indicates that hadron effects in LYSO do not depend on doping level, growth parameters and fine details of its production, as would be the case for different manufacturers.

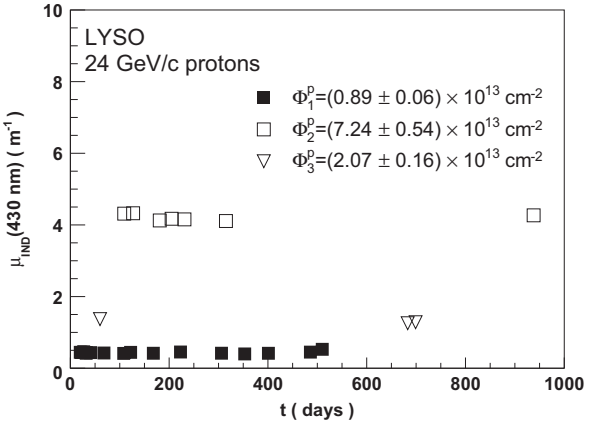

Fig. 5. Induced absorption at the peak-of-emission wavelength of 420 nm, measured longitudinally through the 100 mm length of each crystal at different time intervals after each of the three irradiations. The systematic scale uncertainty on the measurements is 0.08 m^{-1}.

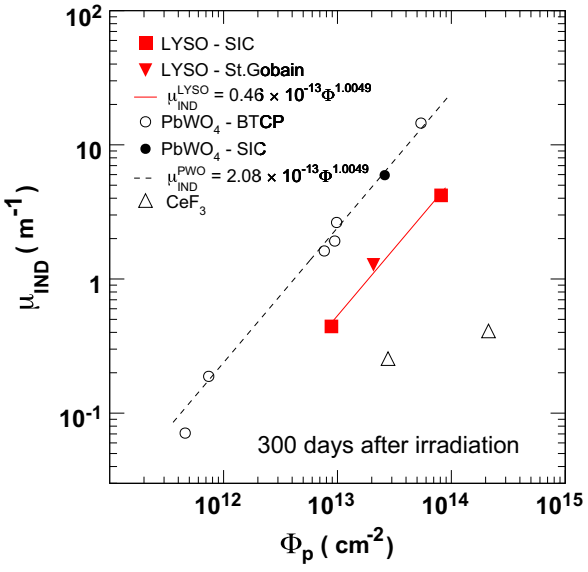

Fig. 6. Induced absorption at the peak-of-emission wavelength for LYSO, measured longitudinally through the crystals, as a function of integrated proton fluence. The systematic uncertainty on the measurements for LYSO is 0.08 m^{-1}. For comparison, existing measurements are shown for $PbWO_4$ from two different producers, SIC and the Bogoroditsk Techno-Chemical Plant (BTCP) [1], and for CeF_3 [5].

6. Radioactivation

The remnant radioactivity after hadron irradiation is relevant in the case of a human intervention after the detector containing such crystals has been operated. Since the fluences in this test have been delivered to the samples over very few hours compared to the duration of LHC running, the absolute values measured here are not relevant for what would be observed in situ. However, the comparison between different crystal types is crucial to anticipate the expected exposure.

As a first step, the induced ambient-dose equivalent rate ("dose") $\dot{H}^*(10)_{ind}$ has been measured with a dose-rate meter AUTOMESS 6150AD5 [30] at 5.7 cm distance from the middle of the SIC sample at various times after the first irradiation. The measurements, rescaled to a fluence $\Phi_p = 10^{13}$ p cm^{-2}, are plotted in Fig. 7. A FLUKA simulation has been performed for the same irradiation (version 2011.2b.3 [31,32]), and its results are plotted in Fig. 7 as well. In the FLUKA description of the irradiation setup, one had to take into account that the proton-induced hadronic shower within the crystal can lead to very forward-directed particles hitting the beam dump of the irradiation zone in the T7 facility. To include possibly backscattered neutrons, the back wall of the irradiation zone, which consists of 20 cm marble and 48 cm of iron yoke, was included in the geometry setup, whereas the side walls were neglected. In the simulation, the Cerium-doped LYSO crystal with dimensions $25 \times 25 \times 100$ mm^3 was exposed to a square-shaped, uniform beam (5×5 cm^2) of 24 GeV c^{-1} protons with an integrated fluence of $\Phi_p = 10^{13}$ p cm^{-2}. To enable the physics models optimised for activation studies in FLUKA, precise

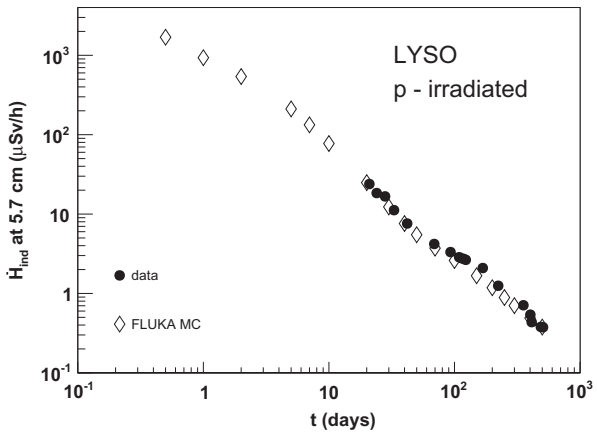

Fig. 7. Measurements of induced ambient-dose equivalent rate as a function of time after the first irradiation, starting 20 days after irradiation, and taken at 5.7 cm from the side of the SIC crystal, compared to FLUKA simulations. The comparison is performed with data and simulations scaled to a fluence $\Phi_p = 10^{13}$ p cm^{-2}. The measurements are affected by a relative scale uncertainty of 7% due to the precision of fluence determination.

thresholds for the particle transport were applied. The transport and production thresholds for electromagnetically interacting particles were set to 100 keV for electrons and positrons, and to 10 keV for photons. The low-energy neutron transport down to thermal energies (10^{-5} eV) was included, as well as the coalescence and the evaporation of heavy fragments. Every other particle created in the shower was transported down to 100 keV. The simulation of the radiation spectrum was optimised for decay radiation, thus the electromagnetic cascade of the prompt radiation was suppressed in the simulation, since it does not contribute to the remnant activation. The ambient-dose equivalent rate $\dot{H}^*(10)_{\mathrm{ind}}$ of the single crystal was simulated in an area with low background—to reflect the measurement conditions in the laboratory—and recorded at a distance of 5.7 cm from the middle of the crystal side, according to the experimental setup. For the calculation, the respective conversion coefficients were used [33]. A very good agreement can be observed in Fig. 7, between FLUKA simulations and measurements, over one and a half years and over two orders of magnitude in dose, with the simulation results falling slightly on the low side. Uncertainties in the comparison can arise from the limited knowledge of Lutetium cross-sections in FLUKA, and from non-uniformities of the beam intensity during irradiation combined with the self-shielding of the crystal. The comparison benchmarks the reliability and predictive power of FLUKA for LYSO crystals.

In a second step, the FLUKA simulations have been extended to full-size crystals, as could be used for a homogenous calorimeter at the HL-LHC collider. In this case, it is relevant to compare the expected remnant radioactivity among crystals of similar dimensions in terms of radiation lengths, typical for such a calorimeter, for an exposure to particles of same energy. For this second simulation, we considered 20 GeV c^{-1} protons, since irradiations and measurements for $PbWO_4$ were performed at this energy, and the comparison has been performed again for an integrated fluence of $\Phi_p = 10^{13}$ p cm^{-2}. The crystal length was $26X_0$, which corresponds to 30 cm for LYSO and 23 cm for $PbWO_4$, while we kept the same transverse dimensions for both crystal types (24×24 mm^2). The ambient dose equivalent rate $\dot{H}^*(10)_{\mathrm{ind}}$ for each crystal was recorded as described above and is depicted in Fig. 8. The FLUKA simulations for LYSO show a remnant dose similar to the one for $PbWO_4$, with the simulation results for $PbWO_4$ lying less than a factor 2 below the measurements. This is an indication that LYSO might become sightly more radioactive than $PbWO_4$ in a $26X_0$ deep calorimeter.

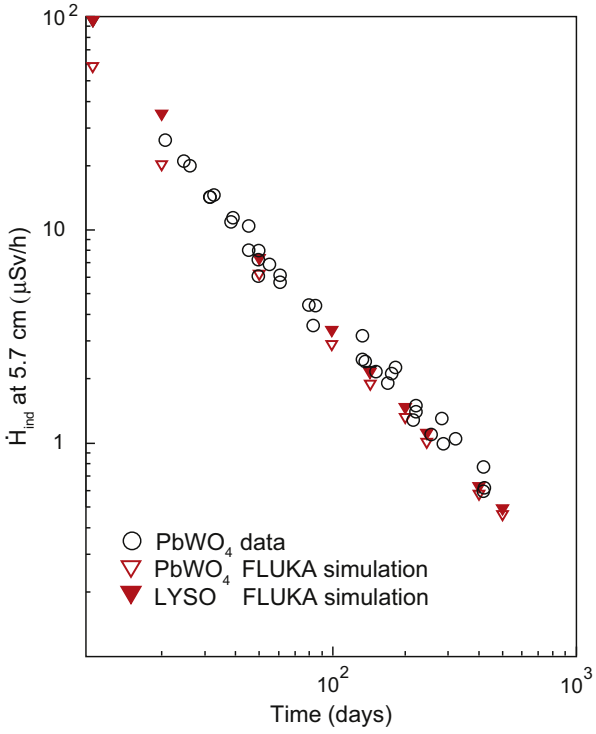

Fig. 8. Induced ambient-dose equivalent rate at 5.7 cm distance from the side of the crystal as a function of time after irradiation calculated with FLUKA for a LYSO crystal exposed to a fluence $\Phi_p = 10^{13}$ p cm^{-2} of 20 GeV c^{-1} protons compared to data and simulations for $PbWO_4$ from Ref. [1] for the same irradiation conditions (all crystals 26 X_0 long). The uncertainties are discussed in the text.

7. Conclusions

Exposure to energetic hadrons of LYSO crystal samples causes a loss in light transmission, that is cumulative, with no sign of recovery over time at room temperature. After an irradiation with 24 GeV c^{-1} protons up to a fluence $\sim 7 \times 10^{13}$ cm^{-2}, an induced absorption coefficient of 4 m^{-1} is observed at the peak-of-scintillation-emission wavelength of 430 nm, almost five times smaller than what observed for $PbWO_4$ exposed to the same irradiation conditions. Proton irradiations at different fluences, and for different sample manufacturers, give the same damage ratio compared to $PbWO_4$. This indicates that hadron-induced damage is independent from the manufacturer, and thus also from fine growth and composition details. The expected remnant radioactivity is of the same order of magnitude as for $PbWO_4$. The damage observed is cumulative, albeit a factor 5 smaller in amplitude than for $PbWO_4$. Whether the material is appropriate for calorimetry in HL-LHC running, will have to be evaluated taking into account the envisaged detector geometry, since the path that scintillation light will have to travel will also play a role.

References

[1] M. Huhtinen, P. Lecomte, D. Luckey, F. Nessi-Tedaldi, F. Pauss, Nuclear Instruments and Methods in Physics Research Section A 545 (2005) 63.
[2] P. Lecomte, D. Luckey, F. Nessi-Tedaldi, F. Pauss, Nuclear Instruments and Methods in Physics Research Section A 564 (2006) 164.
[3] P. Lecomte, D. Luckey, F. Nessi-Tedaldi, F. Pauss, D. Renker, Nuclear Instruments and Methods in Physics Research Section A 587 (2008) 266.
[4] G. Dissertori, D. Luckey, F. Nessi-Tedaldi, F. Pauss, R. Wallny, R. Spikings, R. Van der Lelij, G. Arnau Izquierdo, Nuclear Instruments and Methods in Physics Research Section A 684 (2012) 57.
[5] G. Dissertori, P. Lecomte, D. Luckey, F. Nessi-Tedaldi, F. Pauss, Th. Otto, S. Roesler, Ch. Urscheler, Nuclear Instruments and Methods in Physics Research Section A 622 (2010) 41.
[6] The CMS Electromagnetic Calorimeter Group, P. Adzic et al., Journal of Instrumentation 5 (2010), P03010.
[7] F. Nessi-Tedaldi, Response evolution of the CMS ECAL and R&D studies for electromagnetic calorimetry at the High-Luminosity LHC, in: Proceedings of IEEE NSS Symposium 2012 (Anaheim, USA), paper N35-4 and CMS Conference Report CR-2012/296, CERN, Geneva, Switzerland.
[8] F. Nessi-Tedaldi, Journal of Physics: Conference Series 160 (2009) 012013.
[9] A.S. Iljinov, M.V. Mebel, C. Guaraldo, V. Lucherini, E. De Sanctis, N. Bianchi, P. Levi Sandri, V. Muccifora, E. Polli, A.R. Reolon, P. Rossi, S. Lo Nigro, Physical Review C 39 (1989) 1420.
[10] M. Kobayashi, et al., Nuclear Instruments and Methods 206 (1983) 107.
[11] F. Nessi-Tedaldi, International Journal of Modern Physics A 20 (2005) 3826.
[12] A. Barysevich, V. Dormenev, A. Fedorov, M. Glaser, M. Kobayashi, M. Korjik, F. Maas, V. Mechinski, R. Rusack, A. Singovski, R. Zoueyski, Nuclear Instruments and Methods in Physics Research Section A 701 (2013) 231.
[13] A.H. Gomes, et al., Materials Research Bulletin 4 (1969) 643.
[14] C. Melcher, US Patent, No. 4958080, 1990.
[15] C. Melcher, J. Schweitzer, IEEE Transactions on Nuclear Science NS-39 (1992) 502.
[16] D.W. Cooke, et al., J. Appl. Phys. 88 (2000) 7360;
T. Kimble, et al., in: Proceedings of IEEE on Nuclear Science Symposium, 2002.
[17] Shanghai Institute of Ceramics, Shanghai, 1295 Ding Xi Road, 200050 Shanghai, P. R. China.
[18] C. Wu, Shanghai Institute of Ceramics, Shanghai, 1295 Ding Xi Road, 200050 Shanghai, P. R. China, private communication.
[19] St. Gobain Crystals, 77794 Nemours, France.
[20] J. Chen, L.Y. Zang, R.Y. Zhu, IEEE Transactions on Nuclear Science NS-52 (2005) 3133, and refs. therein.

[21] R. Mao, L.Y. Zang, R.Y. Zhu, IEEE Transactions on Nuclear Science NS-55 (2008) 1759, and refs. therein.
[22] R. Mao, L.Y. Zang, R.Y. Zhu, IEEE Transactions on Nuclear Science NS-59 (2012) 2224.
[23] PreLude420 scintillation material data sheet, St. Gobain Crystals, 77794 Nemours, France.
[24] R. Mao, L.Y. Zang, R.Y. Zhu, IEEE Transactions on Nuclear Science NS-54 (2007) 1319.
[25] M. Thiel, W.M. Döring, V. Dormenev, P. Drexler, R.W. Novotny, M. Rost, A. Thomas, IEEE Transactions on Nuclear Science NS-55 (2008) 1425.
[26] J. Chen, R. Mao, L. Zhang, R.-Y. Zhu, IEEE Transactions on Nuclear Science NS-54 (2007) 718.
[27] M. Glaser, L. Durieu, F. Lemeilleur, M. Tavlet, C. Leroy, P. Roy, Nuclear Instruments and Methods in Physics Research Section A 426 (1999) 72.
[28] The CMS Collaboration, The CMS Electromagnetic Calorimeter Technical Design Report, CERN/LHCC 97-33, CMS TDR 4, CERN, Geneva, Switzerland, 1997.
[29] Perkin-Elmer, Waltham, MA, USA.
[30] Gebrauchsanweisung für den Dosisleistungsmesser 6150AD6, Automation und Messtechnik AG, Ladenburg, Germany, 2001.
[31] G. Battistoni, et al., AIP Conference Proceeding 896 (2007) 31-49; A. Fasso, A. Ferrari, J. Ranft, P.R. Sala, FLUKA: a multi-particle transport code, CERN-2005-10 (2005), INFN/TC 05/11, SLAC-R-773.
[32] G. Battistoni, S. Muraro, P.R. Sala, F. Cerutti, A. Ferrari, S. Roesler, A. Fasso, J. Ranft, The FLUKA code: Description and benchmarking, in: Proceedings of the Hadronic Shower Simulation Workshop 2006, Fermilab, 6–8 September 2006; M. Albrow, R. Raja (Eds), AIP Conference Proceeding, vol. 896, 2007, pp. 31–49.
[33] S. Roesler, G R. Stevenson, deq99.f – a FLUKA user-routine converting fluence into effective dose and ambient dose equivalent, CERN-SC-2006-070-RP-TN, 2006.